Contents lists available at ScienceDirect

Physics Letters B

www.elsevier.com/locate/physletb

PHYSICS LETTERS B
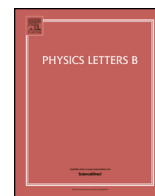
Detecting the upturn of the solar ^{8}B neutrino spectrum with LENA

R. Möllenberg [a,*], F. von Feilitzsch [b], D. Hellgartner [b], L. Oberauer [b], M. Tippmann [b],
J. Winter [c], M. Wurm [c], V. Zimmer [b]

[a] Excellence Cluster Universe, Technische Universität München, 85748 Garching, Germany
[b] Physik Department, Technische Universität München, 85748 Garching, Germany
[c] Institut für Physik, Excellence Cluster PRISMA, Johannes Gutenberg Universität Mainz, 55128 Mainz, Germany

ARTICLE INFO

ABSTRACT

LENA (**L**ow **E**nergy **N**eutrino **A**stronomy) has been proposed as a next generation 50 kt liquid scintillator detector. The large target mass allows a high precision measurement of the solar ^{8}B neutrino spectrum, with an unprecedented energy threshold of 2 MeV. Hence, it can probe the MSW-LMA prediction for the electron neutrino survival probability in the transition region between vacuum and matter-dominated neutrino oscillations. Based on Monte Carlo simulations of the solar neutrino and the corresponding background spectra, it was found that the predicted upturn of the solar ^{8}B neutrino spectrum can be detected with 5σ significance after 5 years.

1. Introduction

The MSW-LMA prediction for the survival probability of solar electron neutrinos $P_{ee}(E_\nu)$ has been confirmed in the energy region of vacuum ($E_\nu \lesssim 1$ MeV) [1–3] and matter dominated oscillations ($E_\nu \gtrsim 5$ MeV) [4–6]. Nevertheless, the predicted low energy upturn of the electron neutrino survival probability (P_{ee}) in the transition region between vacuum and matter dominated oscillations could not be detected, as Water–Čerenkov detectors (WCDs) have a too high energy threshold and current liquid scintillator detectors (LSDs) are too small. A test of the MSW-LMA prediction in the transition region is important as new physics, like non-standard neutrino interactions [7,8] or light sterile neutrinos ($m_{\nu_1} < m_{\nu_0} < m_{\nu_2}$, where the sterile neutrino ν_s is mainly present in the mass eigenstate ν_0) [9], could influence P_{ee} in this region.

Compared to current solar neutrino detectors, the advantage of the proposed LENA detector [10] is the combination of a ~ 200 keV energy threshold and a huge target mass. Thus, the external gamma background, which currently prevents a measurement of the solar ^{8}B spectrum below 3 MeV in Borexino [4], can be suppressed by self-shielding. This enables the measurement of the ^{8}B spectrum with an unprecedented threshold of 2 MeV. Hence, LENA can probe the MSW-LMA prediction over a large part of the transition region.

The present work discusses the sensitivity of LENA to detect the predicted upturn of P_{ee} at low energies by measuring the solar ^{8}B spectrum. In Section 2 the planned detector setup is briefly presented. The simulation of the expected solar neutrino and background spectra is discussed in Section 3 and Section 4. The analysis of the simulated data is presented in Section 5. Finally, the detection potential for the low energy upturn of P_{ee} is discussed in Section 6.

2. The LENA detector

The neutrino target consists of ~ 50 kt of liquid scintillator based on linear-akyl-benzene (LAB), that is enclosed in a cylinder with 14 m radius and 96 m height [11]. The emitted light is detected by photomultiplier tubes (PMTs) that are mounted with non-imaging light concentrators (LCs) inside individual pressure encapsulations that are filled with a non-scintillating buffer liquid. The apertures of these optical modules are located at the boundary of the target volume at a radius of 14 m. The corresponding effective optical coverage is ~30%. The radius of the cylindrical concrete tank is 16 m, so that the target volume is shielded by 2 m of liquid scintillator. A muon veto formed by gas detectors is placed above the detector tank and provides auxiliary information for the reconstruction of cosmic muon tracks. In order to identify and reconstruct inclined muon tracks, an instrumented water volume surrounding the tank serves as an active Water–Čerenkov muon veto and shields the target volume from fast neutrons.

The preferred location for the detector is the Pyhäsalmi mine in Finland. The detector cavern is shielded by 1400 m of rock coverage, corresponding to ~ 4000 m water equivalent (w.e.). Hence, the

* Corresponding author.
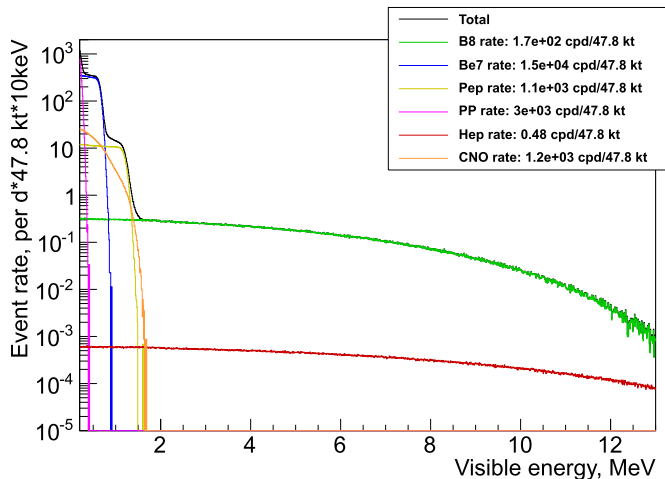 E-mail address: randolph.moellenberg@ph.tum.de (R. Möllenberg).

Fig. 1. The simulated visible energy spectra for solar neutrinos with $P_{ee}(E_\nu)$ according to the MSW-LMA prediction for the ES channel. The spectral shapes of the neutrino fluxes were taken from [18–21]. (For interpretation of the references to color in this figure legend, the reader is referred to the web version of this article.)

cosmic muon flux will be reduced to ~ 0.2 m^{-2}h^{-1} [12], which is about five times less than in Borexino.

3. Simulation of the solar neutrino spectra

There are two possible detection channels for solar ^{8}B neutrinos in LENA. The elastic neutrino electron scattering (ES) channel and charged current reactions of ν_e's on ^{13}C (^{13}C channel) [13,14].

3.1. Elastic neutrino electron scattering

In the ES channel, a neutrino scatters elastically off an electron, which is subsequently detected. As the energy of the recoil electron depends on the scattering angle, the measured recoil spectrum is a convolution of the solar neutrino spectrum and the electron recoil spectrum at a given neutrino energy.

The simulation of the electron recoil spectra was split into two parts. First of all, the differential events rates for neutrinos from different reactions were calculated according to the BS05(AGS, OP) standard solar model [15]. Using these differential events rates, 10^6 electron events were simulated with a GEANT4 [16] based Monte Carlo (MC) simulation of the LENA detector [17]. The events were homogeneously distributed over the target volume, so that possible position dependent effects are considered. Afterwards, the visible energy was reconstructed from the event position and the number of detected photons [17]. The energy resolution is governed by the number of detected photons and amounts to $6.2\% \cdot \sqrt{E/\mathrm{MeV}}$.

Fig. 1 shows the resulting electron recoil spectra. At low energies, the ^{7}Be and the pep neutrinos have the largest event rate, preventing a detection of ^{8}B neutrinos below ~ 1.4 MeV. Above ~ 1.4 MeV, the ^{8}B spectrum is dominant and surpasses the hep spectrum by more than two orders of magnitude.

3.2. Charged current reaction on ^{13}C

The charged current reaction of electron neutrinos on ^{13}C ($\nu_e + {}^{13}\mathrm{C} \rightarrow {}^{13}\mathrm{N} + e^-$) has a threshold of 2.2 MeV. Thus, it is another possible detection channel for solar ^{8}B neutrinos. Due to the kinematics of the reaction, the recoiling ^{13}N nucleus has only a few keV kinetic energy. Hence, the neutrino energy can be reconstructed on an event-by-event basis by measuring the electron energy, taking into account the small effect of the energy resolution of the detector. The subsequent β^+ decay of the ^{13}N nucleus

Table 1
The gamma rates above 250 keV of the different detector components.

	^{40}K	^{238}U chain	^{232}Th chain
Tank	13 MBq	1.1 GBq	178 MBq
PMTs	14 kBq	229 kBq	24 kBq
LCs	0.86 kBq	13 kBq	41 kBq

($\tau = 862$ s) causes a delayed coincidence signal, which can be used to distinguish signal from background events. Hence, ^{13}C events will be selected by the spatial and timing coincidence between prompt and delayed signals. Although the cross section is about 10 times larger than the cross section of the ES channel [14], the event rate is almost two orders of magnitude lower due to the low isotopic abundance of ^{13}C (1.07%). Nevertheless, the measurement of the unconvoluted shape of the solar ^{8}B neutrino spectrum[1] with the ^{13}C channel allows an energy dependent measurement of P_{ee}, as the unoscillated solar ^{8}B flux is known from the NC measurements of the SNO experiment [22].

4. Simulation of the background spectra

There are three different types of background present in the ES channel: external gamma rays that are emitted by the tank, the PMTs and the LCs, cosmogenic radioisotopes produced in-situ by traversing muons and intrinsic radioactive background. A background for the ^{13}C channel is caused by the accidental coincidences of these backgrounds and of ES interactions of solar neutrinos.

Based on the assumed radiopurity of the tank [11], PMTs and LCs [23] (see Table 1), the external gamma ray background was simulated with the GEANT4-based LENA Monte Carlo simulation [17]. It was found that no external gamma background is present above 3.5 MeV. For lower energies, the rate can be reduced to a negligible level by applying a fiducial volume cut. The corresponding fiducial volume is 48 kt above and 19 kt below 3.5 MeV.

Cosmogenic radioisotopes are produced inside the target volume by spallation reactions of cosmic muons on carbon nuclei. The majority of the produced radioisotopes have a lifetime of less than ~ 1 s [4,24]. Hence, the decays can easily be identified by the time coincidence to the parent muon, without introducing a large dead time. The remaining cosmogenic isotopes with a longer lifetime are ^{11}C (β^+), ^{10}C (β^+) and ^{11}Be (β^-) (see Table 2). The spectral shapes of these isotopes were obtained from the GEANT4-based LENA Monte Carlo simulation. Afterwards, the measured rates of the Borexino experiment [4,1] have been scaled to the Pyhäsalmi location, using the muon flux of the two sites.[2] Below 2 MeV, the ^{11}C background is about two orders of magnitude larger than the solar ^{8}B neutrino signal. Hence, the end of the ^{11}C spectrum defines the energy threshold for the detection of solar ^{8}B neutrinos. As ^{10}C and ^{11}Be have a much shorter lifetime than ^{11}C, it is possible to reduce the background from these isotopes by vetoing a cylinder with 2 m radius around each traversing muon for $\Delta t = 4 \cdot \tau(^{10}\mathrm{C}) = 111.2$ s. As the muon rate in the fiducial volume is ~ 135 h^{-1}, the introduced dead time amounts to about 10% of the total exposure, which is still acceptable.

Besides cosmogenic isotopes, there is also a background from intrinsic radioimpurities in the scintillator. As the amount of radioimpurities in the LENA detector is not known at the moment, it was assumed in the following that the radiopurity levels of

---

[1] The spectrum is of course still convoluted with the energy resolution of the detector.

[2] Note that no scaling for the slightly different mean muon energy was applied.

Table 2
List of the cosmogenic radioisotopes with life times above 2 s.

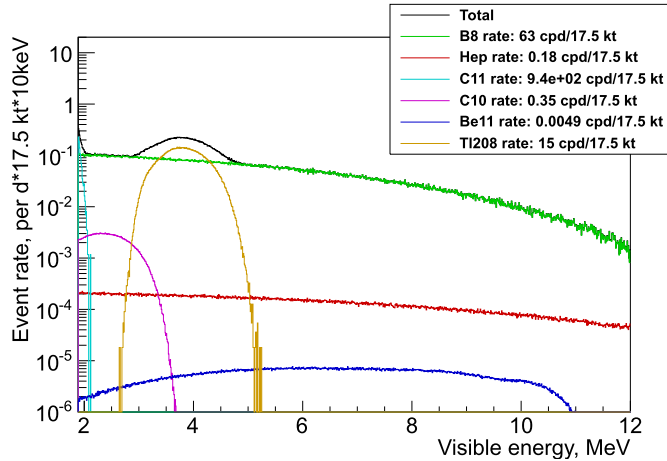| Isotope	Q-value	Life time	Rate [cpd/kt]
^{11}C	2.0 MeV	29.4 min	54
^{10}C	3.7 MeV	27.8 s	1.0
^{11}Be	11.5 MeV	19.9 s	$6.4 \cdot 10^{-2}$

Fig. 2. The simulated visible energy spectra of the cosmogenic and intrinsic radioactive background. A spacial and time cut around each muon was applied to reduce the cosmogenic background and the external gamma background was suppressed to a negligible level by a fiducial volume cut. (For interpretation of the references to color in this figure legend, the reader is referred to the web version of this article.)

the Borexino experiment[3] ($c(^{232}$Th$) = (6.5 \pm 1.5) \cdot 10^{-18}$g/g) [4] are reached. The only intrinsic beta-emitting[4] radioisotopes in the Borexino detector with a Q-value above 2 MeV are ^{214}Bi (^{238}U chain, Q = 3.3 MeV) and ^{208}Tl (^{232}Th chain, Q = 5.0 MeV) [4]. ^{214}Bi can be tagged by the subsequent decay of ^{214}Po and is thus neglected in the following [4]. ^{208}Tl is produced by the alpha decay of ^{212}Bi which also decays into ^{212}Po ($\tau = 0.4$ μs) with 64% branching ratio. Hence, the amount of ^{208}Tl can be determined from the observed number of ^{212}Bi–^{212}Po coincidences. Fig. 2 shows the resulting cosmogenic and intrinsic radioactive background spectra.

Based on these spectra, the accidental background for the ^{13}C channel has been calculated (see Fig. 3) for a fiducial volume of 30 kt. Due to the relatively long life time of the ^{13}N nucleus, a large amount of background is present below 5 MeV reconstructed neutrino energy. The dominant part of the accidental background is due to external gamma rays[5] and cosmogenic ^{11}C events. Above 5 MeV, the accidental background is at least one order of magnitude below the solar ^{8}B signal. Thus, the energy threshold for the ^{13}C channel is set to 5 MeV neutrino energy.

5. Analysis procedure

In order to determine the sensitivity for the detection of the low energy upturn of P_{ee}, the potential to distinguish the MSW-LMA prediction from a simple test model with $P_{ee}(E_\nu) = $const was investigated. Using the previously simulated neutrino and back-

---

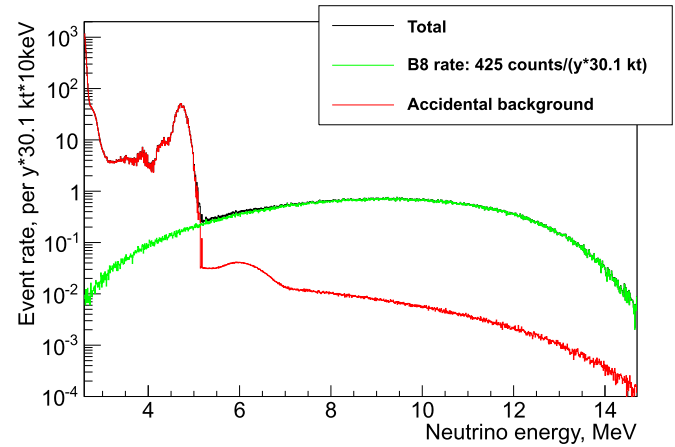[3] Note that the radiopurity levels of the first data taking phase of Borexino are used and that the current radioactive background rates in Borexino have been substantially improved by several purification campaigns.

[4] Alpha emitters above 2 MeV do not pose a background as their light emission is quenched in a liquid scintillator.

[5] Reducing the external gamma background by using a smaller fiducial volume would result in a lower sensitivity to the low energy upturn of P_{ee}, due to the smaller statistics.

Fig. 3. The accidental background spectrum for the ^{13}C channel, using a fiducial volume with 11 m radius. Furthermore, the expected ^{8}B spectrum is shown for comparison. (For interpretation of the references to color in this figure legend, the reader is referred to the web version of this article.)
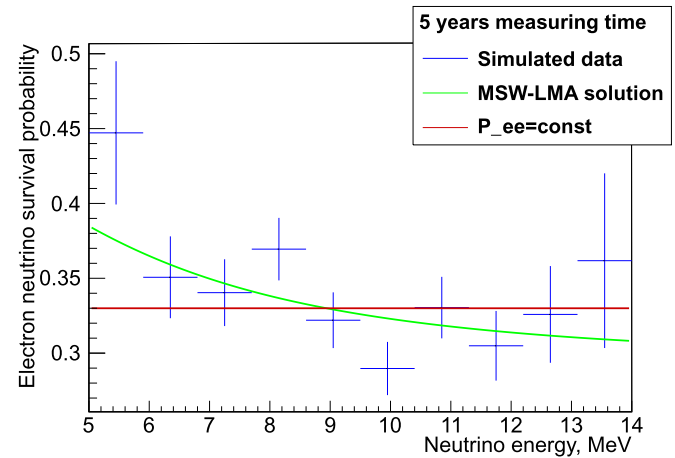

Fig. 4. The measured electron neutrino survival probability after 5 years, using the ^{13}C channel. Furthermore, a fit with the MSW-LMA prediction (depicted in green) and with $P_{ee} = $const (depicted in red) is shown. (For interpretation of the references to color in this figure legend, the reader is referred to the web version of this article.)

ground spectra, 10^5 five year long measurements of the ^{8}B neutrino spectrum were simulated with the ROOT package [25]. Afterwards, the MC data sets were analyzed independently for the ^{13}C channel and the ES channel. The accidental background was subtracted from the ^{13}C channel to retrieve the oscillated solar ^{8}B spectrum. Afterwards, this spectrum was divided by the unoscillated solar ^{8}B spectrum to determine $P_{ee}(E_\nu)$. Note that the accidental background spectrum can be precisely determined from the measured total spectrum of the ES channel. Finally, $P_{ee}(E_\nu)$ was fitted with the MSW-LMA prediction and with the $P_{ee}(E_\nu) = $const model, using a χ^2 minimization. The normalization was treated as a free nuisance parameter in both cases. Hence, this analysis is only sensitive to the shape of $P_{ee}(E_\nu)$ and is thus unaffected by the uncertainty of the solar ^{8}B flux. Fig. 4 shows the result for one example measurement. While the MSW-LMA prediction is preferred one, the statistical significance is not enough to exclude the $P_{ee}(E_\nu) = $const model. Overall, the average exclusion significance in the ^{13}C channel is below 1σ.

For the ES channel, it is not possible to directly calculate P_{ee} from the measured ^{8}B spectrum, as the neutrino energy cannot be reconstructed on an event-by-event basis. Thus, the simulated spectrum was fitted with the expected spectrum according to the
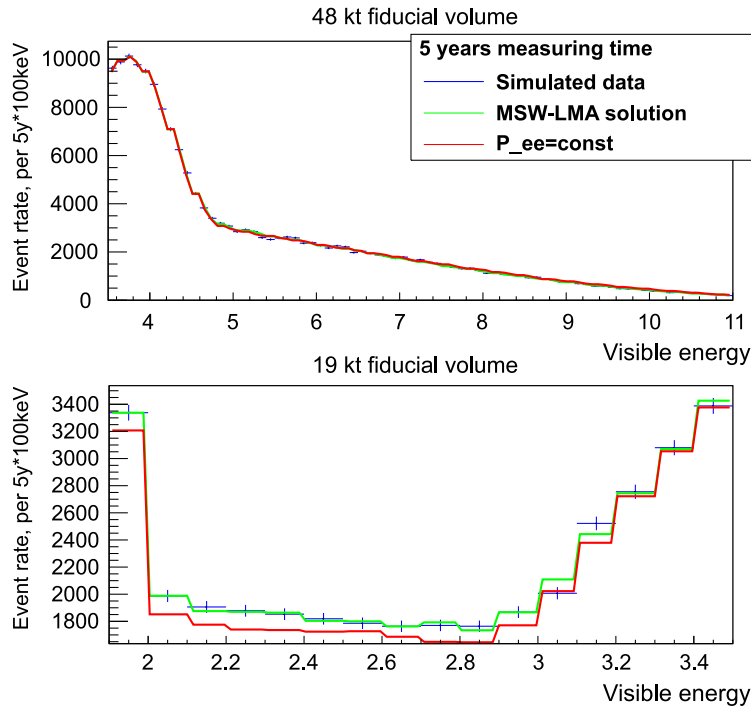
Fig. 5. The total spectrum for the ES channel after 5 years measuring time. Furthermore, a fit according to the MSW-LMA prediction (depicted in green) and according to $P_{ee} = const$ (depicted in red) is shown. (For interpretation of the references to color in this figure legend, the reader is referred to the web version of this article.)

MSW-LMA prediction and the $P_{ee}(E_\nu) = const$ hypothesis, using a χ^2 minimization with free parameters for the solar neutrino and the corresponding background rates. In order to maximize the statistics, the full 48 kt fiducial volume was used above 3.5 MeV, as no external gamma background is present at these energies, while the 19 kt fiducial volume was used below 3.5 MeV. As the contributions of the cosmogenic and intrinsic radioactive background can be measured independently, penalty-terms were added to the χ^2 function to maximize the sensitivity [26]:

$$\chi^2_{tot} = \chi^2 + \chi^2_{pen}, \qquad \chi^2_{pen} = \sum_{j=1}^{k} \frac{(\lambda_j - \mu_j)^2}{\sigma_j^2}, \qquad (1)$$

where k is the number of parameters with prior information, λ_j is the fit value of the parameter j and μ_j is the expected value of the parameter j, with σ_j uncertainty. The uncertainty for the cosmogenic backgrounds was taken from the KamLAND (^{10}C and ^{11}Be) [24] and the Borexino experiment (^{11}C) [1], while the uncertainty for the ^{208}Tl rate was estimated from the expected number of ^{212}Bi–^{212}Po coincidences. Fig. 5 shows the results of the fit for one example measurement. Above ~ 3 MeV visible energy, the data is consistent with both the MSW-LMA prediction and with the $P_{ee} = const$ hypothesis. But below ~ 3 MeV, the MSW-LMA prediction is clearly favored, which shows the importance of measuring the ^{8}B spectrum below 3 MeV, which is not possible with current WC and LS detectors.

In the last step, the results from the ^{13}C and the ES channel were combined by adding the χ^2 values of the corresponding fits. Using these values and the number of degrees of freedom, the probability that the MC data sample is consistent with the MSW-LMA prediction or the $P_{ee}(E_\nu) = const$ model was calculated. In order to suppress statistical fluctuations, this process was repeated for each data sample. Finally, the probability that the $P_{ee}(E_\nu) = const$ model can be excluded with 5σ significance, which is equivalent to a detection of the low energy upturn of P_{ee}, was calculated, assuming that the MSW-LMA prediction is correct.

Table 3
The probability to detect the low energy upturn of P_{ee}, for measuring times ranging from 2 years to 5 years.

Measuring time	Prob. for a 5σ det.
2 years	43.4%
3 years	92.5%
4 years	99.8%
5 years	> 99.9%

6. Results

Table 3 shows the probability for a 5σ detection of the low energy upturn of P_{ee}, as a function of the measurement time. After 2 years, the upturn can be detected at 5σ significance for over 40% of all MC data sets, assuming that the MSW-LMA prediction is correct. After 5 years, the upturn was detected for each data set. Hence, in case that the upturn is not detected after 5 years, the MSW-LMA prediction would be ruled out and new physics must be present that reduce $P_{ee}(E_\nu)$ in the transition region. Comparing the two detection channels, it was found that the sensitivity of the ES channel is much larger than the ^{13}C channel, due to the larger statistics. Nevertheless, the ^{13}C channel still provides an important cross check of the results.

While the amount of cosmogenic background can be precisely estimated for the assumed rock coverage, it is much harder to estimate the intrinsic radioactive background. Hence, the analysis was repeated for a 100 times larger intrinsic radioactive background than in Borexino. Table 4 shows the detection potential for the low energy upturn of P_{ee} in this pessimistic scenario. While the detection potential is of course decreased, the effect of the increased background is not very strong and the upturn can still be detected at 5σ significance after 5 years. The reason for this behavior is that the important energy region below 3 MeV is not affected by the larger ^{208}Tl background. Hence, a precision test of the MSW-LMA prediction is possible with LENA even if radiopurity conditions are substantially worse than in Borexino.

Table 4
The probability to detect the low energy upturn of P_{ee}, for measuring times between 2 years and 5 years and for a 100 times larger intrinsic radioactive background than in Borexino.

Measuring time	Prob. for a 5σ det.
2 years	34.6%
3 years	86.7%
4 years	99.4%
5 years	> 99.9%

7. Conclusions

Present-day experiments lack the capability for a precision measurement of the electron neutrino survival probability P_{ee} in the transition region between vacuum and matter dominated oscillations (1 MeV $\lesssim E_\nu \lesssim$ 5 MeV). LENA will offer an excellent opportunity to close this gap in the determination of P_{ee} by a high-statistics, low-energy-threshold measurement of the solar ^{8}B neutrino spectrum. Due to its large target mass, the external gamma background, that currently prevents a measurement below 3 MeV electron recoil energy in Borexino, can be efficiently suppressed by a stringent fiducial volume cut. This allows a measurement of the solar ^{8}B neutrino spectrum with an unprecedented energy threshold of 2 MeV.

In the present work, the detection potential for the low energy upturn of P_{ee} that is predicted by the MSW-LMA solution was analyzed. It was found that the upturn can be detected at 5σ significance after 5 years measuring time, even if the intrinsic radiopurity level of the scintillator is two orders of magnitude worse than achieved in Borexino. In case that the low energy upturn of P_{ee} is not found, the measurement would rule out the MSW-LMA prediction and show that new physics decrease P_{ee} in the transition region between vacuum and matter dominated oscillations.

Acknowledgements

References

[1] Borexino Collaboration, Precision measurement of the ^{7}Be solar neutrino interaction rate in Borexino, Phys. Rev. Lett. 107 (2011) 141302, arXiv:1104.1816.
[2] GNO Collaboration, Complete results for five years of GNO solar neutrino observations, Phys. Lett. B 616 (2005) 174–190, arXiv:hep-ex/0504037.
[3] SAGE Collaboration, Measurement of the solar neutrino capture rate with gallium metal, Phys. Rev. C 60 (1999) 055801, arXiv:astro-ph/9907113.
[4] Borexino Collaboration, Measurement of the solar ^{8}B neutrino rate with a liquid scintillator target and 3 MeV energy threshold in the Borexino detector, Phys. Rev. D 82 (2010) 033006.
[5] Super-Kamiokande Collaboration, Solar neutrino measurements in Super-Kamiokande-I, Phys. Rev. D 73 (2006) 112001, arXiv:hep-ex/0508053v2.
[6] SNO Collaboration, Electron energy spectra, fluxes, and day–night asymmetries of ^{8}B solar neutrinos from the 391-day salt phase SNO data set, Phys. Rev. C 72 (2005) 055502, arXiv:nucl-ex/0502021.
[7] H. Minakata, C. Pena-Garay, Solar neutrino observables sensitive to matter effects, Adv. High Energy Phys. 2012 (2012) 349686, arXiv:1009.4869.
[8] A. Friedland, C. Lunadi, C. Pena-Garay, Solar neutrinos as probes of neutrino matter interactions, Phys. Lett. B 594 (2004) 347, arXiv:hep-ph/0402266.
[9] P.C. de Holanda, A.Yu. Smirnov, Solar neutrino spectrum, sterile neutrinos and additional radiation in the Universe, Phys. Rev. D 83 (2011) 113011, arXiv:1012.5627.
[10] M. Wurm, et al., The next-generation liquid-scintillator neutrino observatory LENA, Astropart. Phys. 35 (11) (2012) 685–732, arXiv:1104.5620.
[11] L. Oberauer, P. Pfahler, M. Wurm, LAGUNA-LBNO Liquid Scintillator Specification Document, 2012, unpublished.
[12] V.A. Kudryavtsev, N.J.C. Spooner, J.E. McMillan, Simulations of muon-induced neutron flux at large depths underground, Nucl. Instrum. Methods A 505 (2003) 688–698, arXiv:hep-ex/0303007.
[13] J. Arafune, M. Fukugita, Y. Kohyama, K. Kubodera, ^{13}C as a solar neutrino detector, Phys. Lett. B 217 (1989) 186.
[14] A. Ianni, D. Montanino, F.L. Villante, How to observe ^{8}B solar neutrinos in liquid scintillation detectors, Phys. Lett. B 627 (2005) 38–48, arXiv:physics/0506171.
[15] J.N. Bahcall, A.M. Serenelli, S. Basu, New solar opacities, abundances, helioseismology, and neutrino fluxes, Astrophys. J. 621 (2005) L85–L88, arXiv:astro-ph/0412440.
[16] S. Agostinelli, et al., Geant4 – a simulation toolkit, Nucl. Instrum. Methods 1A 506 (2003) 250–303.
[17] R. Möllenberg, Monte Carlo study of solar ^{8}B neutrinos and the diffuse supernova neutrino background in LENA, PhD thesis, Technische Universität München, 2013.
[18] J.N. Bahcall, The pp solar neutrino energy spectrum, http://www.sns.ias.edu/~jnb/SNdata/ppspectrum.html, accessed: 04.29.2014.
[19] J.N. Bahcall, R.K. Ulrich, Solar models, neutrino experiments, and helioseismology, Rev. Mod. Phys. 60 (1988) 297–372, http://www.sns.ias.edu/~jnb/.
[20] J.N. Bahcall, E. Lisi, D.E. Alburger, L.D. Braeckeleer, S.J. Freedman, J. Napolitano, Standard neutrino spectrum from ^{8}B decay, Phys. Rev. C 54 (1996) 411.
[21] J.N. Bahcall, Hep energy spectrum, http://www.sns.ias.edu/~jnb/SNdata/Export/Hepspectrum/hepspectrum.dat, accessed: 04.29.2014.
[22] The SNO Collaboration, Measurement of the ν_e and total ^{8}B solar neutrino fluxes with the Sudbury neutrino observatory phase-III data set, Phys. Rev. C 87 (2013) 015502.
[23] J. Maneira, Calibration and monitoring for the Borexino solar neutrino experiment, PhD thesis, Universidade de Lisboa, 2001.
[24] KamLAND Collaboration, Production of radioactive isotopes through cosmic muon spallation in KamLAND, Phys. Rev. C 81 (2010) 025807, arXiv:0907.0066.
[25] R. Brun, F. Rademakers, ROOT – an object oriented data analysis framework, Nucl. Instrum. Methods Phys. Res., Sect. A 389 (1997) 81–86, http://root.cern.ch.
[26] K.A. Hochmuth, Low energy neutrinos as geological and astrophysical messengers, PhD thesis, Technische Universität München, 2008.